

A DETAIL STUDY ON THERMAL MANAGEMENT WITH GRAPHENE LATERAL HEAT SPREADERS

KATA SAI KIRAN GOUD, DR.V.ASHOK KUMAR, K.MANOJ

PG Scholar Department of Mechanical Engineering, Mother Theresa College of Engineering & Technology

Associate professor & HOD Department of Mechanical Engineering, Mother Theresa College of Engineering & Technology

Assistant Professor Department of Mechanical Engineering, Mother Theresa College of Engineering & Technology

Abstract: We review the thermal properties of graphene, few-layer graphene and graphene nanoribbons, and discuss practical applications of graphene in thermal management and energy storage. The first part of the review describes the state-of-the-art in the graphene thermal field focusing on recently reported experimental and theoretical data for heat conduction in graphene and graphene nanoribbons. The effects of the sample size, shape, quality, strain distribution, isotope composition, and point-defect concentration are included in the summary. The second part of the review outlines thermal properties of graphene-enhanced phase change materials used in energy storage. It is shown that the use of liquid-phase-exfoliated graphene as filler material in phase change materials is promising for thermal management of high-power-density battery parks. The reported experimental and modeling results indicate that graphene has the potential to outperform metal nanoparticles, carbon nanotubes, and other carbon allotropes as filler in thermal management materials

Keywords: graphene; thermal conductivity; graphene applications; thermal phase change materials

1. Introduction and Terminology

In this paper, we review thermal properties of graphene, few-layer graphene (FLG), and graphene nanoribbons (GNR) and provide an example of a graphene application in thermal phase change materials (PCM). In many cases, when discussing graphene thermal applications, we use the term graphene even when the actual material consists of a mixture of single layer graphene (SLG), bilayer graphene (BLG), and FLG. The latter is because for thermal

applications the difference between SLG and FLG is not as important as for electronic applications. It is sometimes difficult to distinguish between FLG and graphite films or between FLG and graphite nano-platelets (GnP) used in composite materials. The definition of SLG—a single atomic plane of sp²-bound carbon—is strict. The distinction between FLG and thin film of graphite or bulk graphite depends on the context. Investigating electrical properties one can

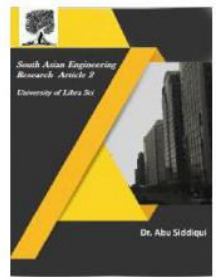


2581-4575

International Journal For Recent Developments in Science & Technology



A Peer Reviewed Research Journal



consider the material to be FLG rather than graphite as long as it is thin enough for changing its carrier density via the electrostatic gating. In the thermal field, one can consider the film to be FLG as long as its Raman spectrum is different from that of bulk graphite.

Acoustic phonons determine the thermal properties of graphene and graphite at room temperature (RT) $T = 300$ K, while the optical phonons define their Raman spectrum [1–5]. In both cases, the crystal lattice dynamics is essential for the distinction between FLG and graphite. The Raman spectrum of FLG differs from that of graphite for the thickness H less than seven to 10 atomic planes [6–11]. In this review, we consider the materials to be FLG when its phonon properties are different from those of graphite ($H \leq 10 \approx 3.5$ nm). In most of cases, FLG flakes have larger lateral sizes (up to a few micrometers) than their thickness H .

The initial interest in the thermal properties of graphene and FLG was driven by the exotic physics of two-dimensional (2D) phonon transport [1–5]. Recently, the studies turned to thermal properties of graphene and related composite materials from the position of practical applications. In this review, we briefly outline the state-of-the-art and new developments in the field of thermal properties of graphene. In addition, as an example of a practical application of graphene in thermal management, we will describe graphene-enhanced phase-change materials (PCMs). Readers interested in details of the phonon

thermal transport in graphene and FLG are referred to other recent reviewers [1–3,12,13].

2. Motivations for Graphene Applications in Thermal Management

Development of high-power-density batteries, e.g., Li-ion batteries, enabled progress in mobile communications, consumer electronics, and automotive industries [14–16]. Temperature rise beyond the normal operating range negatively affects Li-ion battery performance. If overheated, the battery can suffer thermal runaway, cell rupture or explosion [17–19]. A conventional approach for thermal management of high-power-density-ion battery packs is based on the utilization of thermal PCMs. They reduce the temperature rise in the battery due to the latent heat storing and phase changes over a small temperature range [20–22].

The common PCMs have very low thermal conductivity, K , with typical values in the range of 0.17–0.35 W/mK at RT [23]. For comparison, the room-temperature (RT) thermal conductivity of Si and Cu are ~145 W/mK and ~381 W/mK, respectively. Conventional PCMs store heat from the batteries rather than transfer it away from the battery pack. The use of PCM in battery cells also serves the purpose of buffering the battery cell from extreme fluctuations in ambient temperature. This is different from thermal management of computer chips. To reduce the temperature rise in a computer chip, one uses thermal interface materials (TIMs) or heat spreaders that facilitate heat transfer from the chip to the heat sink

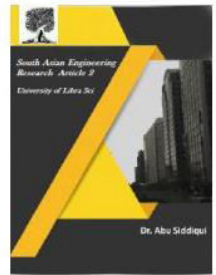


2581-4575

International Journal For Recent Developments in Science & Technology



A Peer Reviewed Research Journal



[15,24,25]. The thermal conductivity of TIMs is in the range of 1–10 W/mK while that of solid graphite-based heat spreaders can be on the order of 1000 W/mK [26]. In this review we describe how these two different approaches for thermal management can be combined via the introduction of the hybrid PCM with graphene acting as filler for increased thermal conductivity. The properties that allow graphene to be an exceptional filler material are its high intrinsic thermal conductivity [1,2], and strong binding with various matrix materials [25,27–30]. The discussion of graphene applications in PCMs will mostly follow our work reported in Ref. [29].

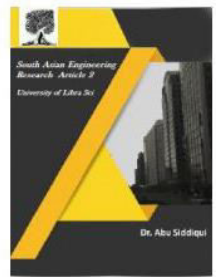
3. Intrinsic Thermal Conductivity of Graphene

We start by summarizing the state of the art in the fundamental understanding of the thermal properties of graphene, focusing on recent theoretical and experimental reports. In 2008, it was discovered at the University of California—Riverside that graphene has extremely high intrinsic thermal conductivity K , which can exceed that of carbon nanotubes (CNTs) [1–5]. FLG retains excellent thermal properties [1,2,31]. Graphite, which is the 3D bulk limit for FLG with the number of layers $n \rightarrow \infty$, is still an outstanding heat conductor with the intrinsic $K \approx 2000$ W/mK at RT. For comparison, $K \approx 430$ W/mK for silver and is much lower for silver nanoparticles used in TIMs. The first experimental studies of thermal conductivity of graphene were carried out using an original non-contact

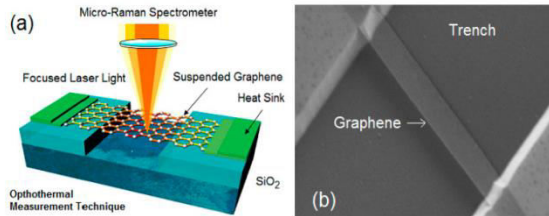
optothermal technique based on Raman spectroscopy (see Figure 1a,b). Taking into account the temperature shift of Raman G-peak, the temperature profiles for large-area suspended graphene flakes were determined. The thermal conductivity values were extracted from numerical simulations, taking into account temperature profiles and actual size and shape of the flakes. It was established that graphene demonstrates very high thermal conductivity K , exceeding 3000 W/mK near RT for large graphene flakes [1–5]. The measurements were performed with large-area suspended graphene layers exfoliated from bulk graphite. The development of the optothermal technique was instrumental for carrying out the thermal measurements with graphene. In the optothermal technique, the heating power, ΔP , is provided with the laser light focused on a suspended graphene layer connected to heat sinks at both ends [1]. The temperature rise, ΔT , in response to the dissipated power, ΔP , is determined with a Raman spectrometer. The Raman G peak in graphene's spectrum exhibits strong temperature, T , dependence. The calibration of the spectral position of G peak with temperature has to be performed by changing the sample temperature while using low laser power to avoid local heating. During the thermal conductivity measurements the suspended graphene layer is heated by the increasing laser power. The local temperature rise in graphene is measured as $\Delta T T = \Delta \omega \omega G G / \phi \phi G G$, where $\phi \phi G G$ is the temperature coefficient of the



2581-4575



Raman G peak in the relevant temperature range [1].



4. Theory of the Thermal Conductivity of Graphene and GNR

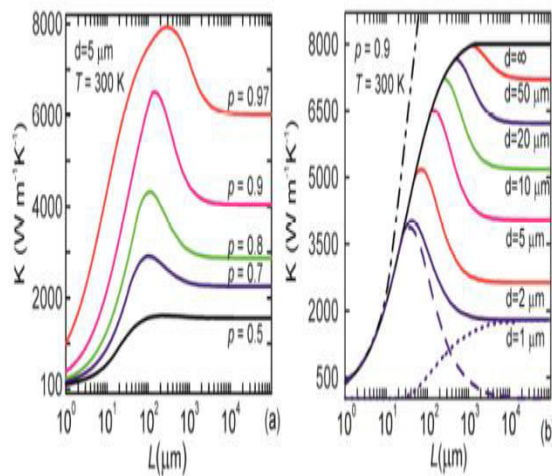
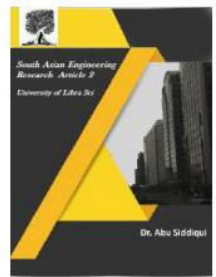
The first experimental investigations of the thermal properties in graphene materials [4,5,31–33,37] stimulated numerous theoretical and computational works in the field (see Figure 2a,b). Here, we briefly review the state-of-the-art in theory of thermal transport in graphene and GNRs. Many different theoretical models have been proposed for the prediction of the phonon and thermal properties in graphite, graphene and GNRs during the last few years. The phonon energy spectra have been theoretically investigated using Perdew-Burke-Ernzerhof generalized gradient approximation (GGA) [38–40], valence-force-field (VFF) and Born-von Karman models of lattice vibrations [41–46], continuum approach [47–49], first-order local density approximation [39,50,51], fifth- and fourth-nearest neighbor force constant approaches [40,52] or utilized the Tersoff, Brenner or Lennard-Jones potentials [53–55]. The thermal conductivity investigations have been performed within molecular dynamics simulations [56–72], density functional theory [73,74], Green's function method [75,76] and Boltzmann-transport-equation (BTE) approach [31,41–

43,49,53–55,77–85]. It has been shown that phonon energies strongly depend on the interatomic force constants (IFCs)—fitting parameters of interatomic interactions, used in the majority of the models. Therefore a proper choice of interatomic force constants is crucial for the accurate description of phonon energy spectra and thermal conductivity in graphene, twisted graphene and graphene nanoribbons [1–3,44,86].

Although various models predicted different values of thermal conductivity, they demonstrated consistent results on the strong dependence of graphene lattice thermal conductivity on the extrinsic parameters of flakes: edge quality, FLG thickness, lateral size and shape, lattice strain, isotope, impurity and grain concentration. The molecular dynamic (MD) simulations usually give smaller values of thermal conductivity in comparison with the BTE model and experimental data due to exclusion of long wavelength phonons from the model by a finite size of the simulation domain [2]. The effect of the edge roughness on the thermal conductivity in graphene and GNRs has been investigated in Refs. [41–43,49,57,79–82,84,85,87,88]. The rough edge can suppress the thermal conductivity by an order of magnitude as compared to that in graphene or GNRs with perfect edges due to the boundary scattering of phonons. Impurities, single vacancies, double vacancies and Stone-Wales defects decrease the thermal conductivity of graphene and GNRs by more than 50%–80% in dependence of the defect concentration [41–43,63–67,79].



2581-4575



A number of studies [68–70] employed the MD simulations to investigate the length dependence of the thermal conductivity in graphene and GNRs. The converged thermal conductivity in graphene was found for $L > 16 \mu\text{m}$ in Ref. [68]. In Refs. [69,70], the thermal conductivity increases monotonically with an increase of the length up to $2.8 \mu\text{m}$ in graphene [70] and 800 nm in GNRs [69]. The obvious length dependence in graphene and GNRs can be attributed to the extremely large phonon mean free path $\Lambda \sim 775 \text{ nm}$ [5], which provides noticeable length dependence even for flakes with micrometer lengths. The available values of phonon thermal conductivity in SLG, few-layer graphene and GNRs are presented in Table 1 at RT (if not indicated otherwise). Readers interested in a more detailed description of theoretical models for the heat conduction in graphene materials are referred to other reviews [2,13].

Table 1. Thermal conductivity of graphene and graphene nanoribbons.

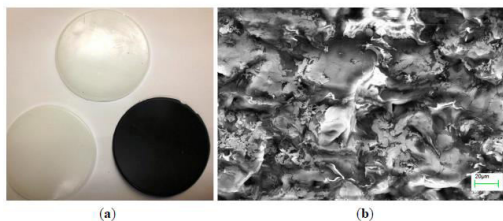
Sample	K (W/mK)	Method	Description	Refs.
Experimental Data				
SLG	~3000–5000	Raman optothermal	Suspended; exfoliated	[4,5]
	2500	Raman optothermal	Suspended; chemical vapor deposition (CVD) grown	[32]
	1500–5000	Raman optothermal	Suspended; CVD grown	[33]
	600	Raman optothermal	Suspended; exfoliated; $T \sim 660 \text{ K}$	[99]
	600	Electrical	Supported; exfoliated	[37]
	310–530	Electrical	Exfoliated and chemical vapor deposition grown; self-heating $T \sim 1000 \text{ K}$	[100]
FLG	1300–2800	Raman optothermal	Suspended; exfoliated; $n = 2-4$	[31]
	50–970	Heat-spreader method	FLG, encased within SiO_2 ; $n = 2, \dots, 21$	[101]
	150–1200	Electrical self-heating	Suspended and supported FLG; polymeric residues on the surface	[102]
	302–596	Modified T-bridge	Suspended; $n = 2-8$	[103]
Bilayer graphene	560–620	Electrical self-heating	Suspended; polymeric residues on the surface	[104]
FLG	1100	Electrical self-heating	Supported; exfoliated; $n < 5$	[105]
nanoribbons	80–150	Electrical self-heating	Supported	[106]

5. Graphene Applications in Thermal Phase-Change Materials

In this section we briefly outline the approach of Balandin and co-workers [29] for graphene's practical applications in thermal PCMs and outline results of other groups that reported the use of graphitic nanoparticles for such applications. As an example material system for the composite matrix we selected a specific paraffin wax. Paraffins or paraffinic hydrocarbons have the general composition of $\text{C}_n\text{H}_{2n+2}$ and are straight-chain or branching saturated organic compounds [110]. Commonly used in PCMs, paraffin waxes have the advantages of low cost and availability, are chemically stable, and are durable to cycling. Paraffins are suitable for the thermal control of batteries with its large range of melting points and a high latent heat of fusion ($\sim 250 \text{ kJ/kg}$). The specific paraffin (IGI-1260) used has a relatively

high melting point of $T_m \sim 70^\circ\text{C}$. The n-alkanes distribution of this paraffin wax predominately consists of C34-C35 hydrocarbons [110]. The paraffin wax is a solid at room temperature and will start to exhibit softening characteristics at elevated temperatures as the long hydrocarbon chains are broken down into smaller ones with the absorption of heat.

Figure 3. Hybrid graphene—paraffin phase change material. (a) Optical image of the PCM samples showing the change in color from white to black with increasing graphene content; (b) Scanning electron microscopy image of the hybrid graphene-PCM indicating uniform distribution of the graphene flakes.

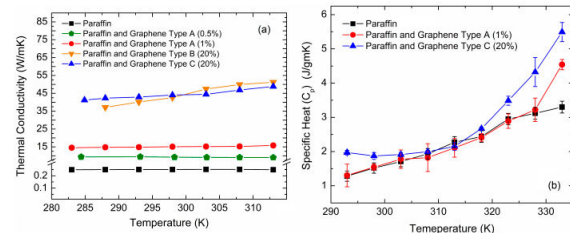


6. Thermal Conductivity of Graphene-Enhanced Phase Change Materials

The transient plane source (TPS) method was used to measure the thermal conductivity of the hybrid composites [119–126]. The results of the measurements were compared to those obtained by other experimental techniques [123–124]. Starting with pristine paraffin as the baseline composite, thermal conductivity was measured at $K = 0.25\text{ W/mK}$. One can see in Figure 4a that as graphene-FLG filler is added to the baseline composite, a drastic increase of K is observed. The hybrid graphene-PCM composite with a 1 wt. % loading fraction possesses a measured thermal conductivity of $\sim 15\text{ W/mK}$ at RT. This represents a significant increase in thermal conductivity by a factor of 60. This thermal conductivity enhancement factor, defined by $\varepsilon = (K - K_m)/K_m$, where K is

the measured thermal conductivity of the composite and K_m is the thermal conductivity of the paraffin matrix, is exceptionally high compared with values reported for either PCMs with fillers [127–129] or TIMs [26,28,30]. The trend continues up to a graphene loading fraction of 20 wt. % where the composite yields the highest value of thermal conductivity at $\sim 45\text{ W/mK}$, an enhancement of more than two orders of magnitude. Figure 4a presents the enhancement factors of thermal conductivity among the pristine paraffin wax and hybrid graphene-PCM composites with different graphene-FLG loading fractions [29].

Figure 4. Thermal properties of hybrid graphene-PCM. (a) Enhancement factor of thermal conductivity of the graphene—paraffin composites with different graphene loading as a function of temperature. The results for pristine paraffin are also shown for comparison; (b) Specific heat of the composites and reference pristine paraffin as a function of temperature. The image is reprinted with permission from [29]. Copyright 2014 Elsevier.



Thermal coupling in the case between graphene fillers and paraffin matrix is likely to be stronger than other matrix-filler combinations. The density function theory (DFT) calculations and molecular dynamics (MD) simulations indicated a possibility of strong increase of the thermal conductivity in ordered graphene composites with organic matrix where the heat transport is along the direction of the graphene atomic planes. Enhancements of up to $K/K_m \approx 360$ have been reported for a graphene loading of 5% [135]. The exceptionally strong anisotropic increase in K was attributed to

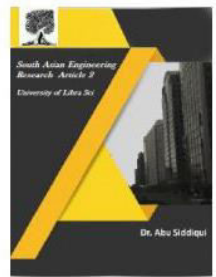


2581-4575

International Journal For Recent Developments in Science & Technology



A Peer Reviewed Research Journal



graphene's planar geometry and good coupling to the octane molecules [135–137]. The heat carrying phonon modes excited in graphene coupled well to those in the organic molecules of the matrix material. Although a direct comparison between the experimental data for the graphene-paraffin composite and the composite studied in Ref. [135] theoretically is not possible, one can conclude that even randomly oriented graphene flakes should produce a strong increase in the thermal conductivity of composites. The dependence of thermal conductivity to a wide temperature range is relatively weak in all hybrid graphene-PCM composites, providing additional benefits for practical PCM-based applications. The opportunities for improvement in such thermal management applications can be obtained only if increasing thermal conductivity will not degrade the inherent latent heat storage properties of PCMs. Figure 4b presents the specific heat data in the examined temperature range.

7. Application of Graphene-Enhanced PCMs in Battery Packs

In this section we give an example of a specific practical application using graphene-enhanced PCMs as energy storage for thermal management in battery packs [29]. The goal in this application was to increase PCM's thermal conductivity without degrading its latent heat storage ability. The battery packs consisted of cylindrical Li-ion batteries connected to a charging-discharging setup that delivered continuous charging-discharging cycles of 16A and 5A, respectively. During the pre-set

ten charge-discharge cycles, temperature measurements were logged at assigned time intervals using strategically placed thermocouples and a data acquisition system (DAS). Two thermocouples were attached to the cathode and anode ends of a battery cylinder inside of the battery pack; a third thermocouple was attached to the battery pack shell that was acting as the heat sink; and a fourth thermocouple exposed to the ambient environment. The battery packs themselves were prepared with different media, including air (i.e., no PCM), pristine paraffin PCM, and hybrid graphene-PCM with different graphene loading fractions. The paraffin PCM used in these battery packs was melted, mixed with graphene solutions (as applicable), and allowed to cool to RT before testing. All experiments followed the same test and setup protocols. The representative results of the tests of the hybrid graphene-PCM reported by Balandin and co-workers [29] are presented in Figure 5.

8. Modeling-Based Optimization of Thermal Management with Graphene-Enhanced PCMs

Computer simulation of thermal management systems for battery packs provides valuable information for materials and system optimization. We corroborated our experimental results with the numerical solution defined by the heat diffusion equation for transient conductive heat transfer in solids and parametric data of the empirical battery design. These parameters along with the measured specific heat and thermal conductivity properties of the

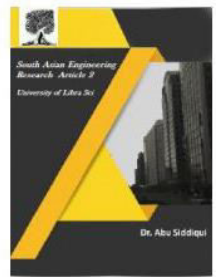


2581-4575

International Journal For Recent Developments in Science & Technology



A Peer Reviewed Research Journal



synthesized composites were used to model the conductive heat flow in the Li-ion battery pack using COMSOL's computer simulation software package. The constructed three-dimensional (3D) model facilitated the analysis of the six-cylinder battery pack in different media. The six batteries, 18.4 mm in diameter, were evenly distributed within a medium represented as a solid cylinder, 70 mm in diameter, all of which were enclosed within a 1 mm thick aluminum sheath. Due to the battery pack's simple construction, an extra coarse mesh of free tetrahedrals was used for the solid cylinders, heat conductive medium within which the solid cylinders were encased, and aluminum sheath. The transient conductive heat transfer equation was solved to determine the temperature rise inside and outside of the battery pack [29]. In all simulation runs only the material characteristics of the medium that fill the space among the battery cylinders were modified. The different media included air, conventional paraffin PCM, and graphene-enhanced PCM. For conventional paraffin PCM without graphene we used thermal conductivity $K = 0.25 \text{ W/mK}$, mass density 900 kg/m^3 , and heat capacity 2500 J/kgK . The simulation results included a transient analysis of temperature vs. time for any specific point inside the 3D modeled battery pack at any given time. Specific locations of the data analyzed correspond to the physical placement of thermocouples in the empirical test setup.

9. Conclusions

In this paper we presented a review of the thermal properties of graphene and few-layer graphene. The results of the experimental and theoretical studies of thermal conductivity at room temperature and above are summarized in a comprehensive table. The practical applications of graphene in thermal management are outlined in an example using thermal phase change materials. It is shown that the use of liquid-phase-exfoliated graphene as filler material in phase change materials is promising for thermal management of high-power battery packs. The described results indicate that graphene has the potential to outperform metal nanoparticles and carbon allotropes as filler in materials for thermal management.

References

1. Balandin, A.A. Thermal properties of graphene and nanostructured carbon materials. *Nat. Mater.* 2011, 10, 569–581.
2. Nika, D.L.; Balandin, A.A. Two-dimensional phonon transport in graphene. *J. Phys.* 2012, 24, 233203.
3. Balandin, A.A.; Nika, D.L. Phonons in low-dimensions: Engineering phonons in nanostructures and grapheme. *Mater. Today* 2012, 15, 266–275.
4. Balandin, A.A.; Ghosh, S.; Bao, W.; Calizo, I.; Teweldebrhan, D.; Miao, F.; Lau, C.N. Superior thermal conductivity of single layer grapheme. *Nano Lett.* 2008, 8, 902–907.
5. Ghosh, S.; Calizo, I.; Teweldebrhan, D.; Pokatilov, E.P.; Nika, D.L.; Balandin, A.A.; Bao, W.; Miao, F.; Lau, C.N. Extremely

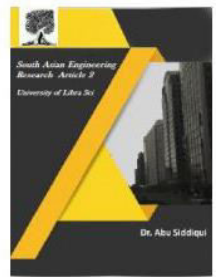


2581-4575

International Journal For Recent Developments in Science & Technology



A Peer Reviewed Research Journal



high thermal conductivity in graphene: Prospects for thermal management application in nanoelectronic circuits. *Appl. Phys. Lett.* 2008, 92, 151911.

6. Ferrari, A.C.; Meyer, J.C.; Scardaci, V.; Casiraghi, C.; Lazzeri, M.; Mauri, F.; Piscanec, S.; Jiang, D.; Novoselov, K.S.; Roth, S.; et al. Raman Spectrum of Graphene and Graphene Layers. *Phys. Rev. Lett.* 2006, 97, 187401.

7. Calizo, I.; Balandin, A.A.; Bao, W.; Miao, F.; Lau, C.N. Temperature Dependence of the Raman Spectra of Graphene and Graphene Multilayers. *Nano Lett.* 2007, 7, 2645–2649.

8. Calizo, I.; Miao, F.; Bao, W.; Lau, C.N.; Balandin, A.A. Variable temperature Raman microscopy as a nanometrology tool for graphene layers and graphene-based devices. *Appl. Phys. Lett.* 2007, 91, 071913.

9. Calizo, I.; Bao, W.; Miao, F.; Lau, C.N.; Balandin, A.A. The effect of substrates on the Raman spectrum of graphene: Graphene-on-sapphire and graphene-on-glass. *Appl. Phys. Lett.* 2007, 91, 201904.

10. Calizo, I.; Bejenari, I.; Rahman, M.; Liu, G.; Balandin, A.A. Ultraviolet Raman microscopy of single and multilayer graphene. *J. Appl. Phys.* 2009, 106, 043509.

11. Teweldebrhan, D.; Balandin, A.A. Modification of graphene properties due to electron-beam irradiation. *Appl. Phys. Lett.* 2009, 94, 013101.

12. Sadeghi, M.M.; Pettes, M.T.; Shi, L. Thermal transport in graphene. *Solid State Commun.* 2012, 152, 1321–1330.

13. Wemhoff, A.P. A review of theoretical techniques for graphene and graphene nanoribbons thermal conductivity prediction. *Int. J. Transp. Phenom.* 2012, 13, 121.

14. Balandin, A. Better computing through CPU cooling. *IEEE Spectr.* 2009, 29, 35–39.

15. Garimella, S.V.; Fleischer, A.S.; Murthy, J.Y.; Keshavarzi, A.; Prasher, R.; Patel, C.; Bhavnani, S.H.; Venkatasubramanian, R.; Mahajan, R.; Joshi, Y.; et al. Thermal Challenges in Next-Generation Electronic Systems. *IEEE Trans. Compon. Packag. Technol.* 2008, 31, 801–815.

16. Linden, D.; Reddy, B.T. *Handbook of Batteries*; McGraw-Hill: New York, NY, USA, 2002.

17. Spotnitz, R.; Franklin, J. Abuse behavior of high-power, lithium-ion cells. *J. Power Sources* 2003, 113, 81–100.

18. Mikolajczak, C.; Kahn, M.; White, K.; Long, R.T. *Lithium-Ion Batteries Hazard and Use Assessment*. *Fire Prot. Res. Found.* 2011, 76, 102.

19. FAA Press Release. Federal Aviation Administration; FAA Press: Washington, DC, USA, 2013.

20. Zalba, B.; Marin, J.M.; Cabeza, L.F. Review on thermal energy storage with phase change: Materials, heat transfer analysis and applications. *Appl. Ther. Eng.* 2003, 23, 251–283.

21. Agyenim, F.; Hewitt, N.; Eames, P.; Mervyn, S. A review of materials, heat transfer and phase change problem formulation for latent heat thermal energy

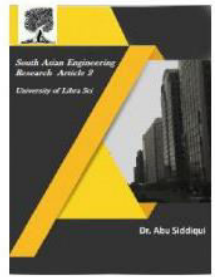


2581-4575

International Journal For Recent Developments in Science & Technology



A Peer Reviewed Research Journal



- storage systems (LHTESS). *Renew Sustain. Energy Rev.* 2010, 14, 615–628.
22. Farid, M.M.; Khudhair, A.M.; Razack, S.A.; Al-Hallaj, S. A review on phase change energy storage: Materials and applications. *Energy Convers. Manag.* 2004, 45, 1597–1615.
23. Sharma, S.D.; Sagara, K. Latent heat storage materials and systems: A review. *J. Green Energy* 2005, 2, 1–56.
24. Yu, A.; Ramesh, P.; Itkis, M.E.; Bekyarova, E.; Haddon, R.C. Graphite nanoplatelet-epoxy composite thermal interface materials. *J. Phys. Chem. C* 2007, 111, 7565–7569.
25. Prasher, R. Thermal conductivity of composites of aligned nanoscale and microscale wires and pores. *Proc. IEEE* 2006, 94, 1571–1585.